

NEW SPECTROSCOPIC BINARIES WITH GAIA AND THE GAIA-ESO SURVEY

M. Van der Swaelmen¹, T. Merle², S. Van Eck² and A. Jorissen²

Abstract. The Gaia-ESO Survey (GES) is a large public spectroscopic survey which acquired spectra for more than 100000 stars across all major components of the Milky Way. Using the 161000 GIRAFFE spectra obtained by GES and corresponding to more than 37000 Milky Way field star objects, we compute cross-correlations functions (CCF) to hunt for spectroscopic binaries (SB) with one, two or more stellar components visible in their spectra. We design cross-correlating templates (named Nacre) to improve the SB detection efficiency at medium-resolution, and in particular, in the near-infrared Calcium II triplet region. Thanks to this optimisation, the CCFs are narrower and allow to unblend more stellar components than standard masks. We then analyse the Nacre CCFs with the extremum-finding tool Doe to measure the radial velocities of each detected stellar component. We will show how the Nacre CCFs have improved the number of detected SB2 by a factor 1.5 compared to our previous analysis. With the help of the Nacre CCFs, we identify 322 SB2, ten SB3 and two SB4 in the examined sample. We will discuss the locus of the SB2, SB3 and SB4 in the Gaia colour-magnitude diagram, provide an estimate of the SB2 frequency and characterise the mass-ratio distribution of the uncovered SB2. All the results of this study are presented in Van der Swaelmen et al. (2023).

Keywords: (stars:) binaries: spectroscopic – (stars:) binaries (including multiple): close – techniques: spectroscopic – techniques: radial velocities

1 Introduction and data selection

Spectroscopic surveys have revealed many spectroscopic binaries (SB) candidates. SBs with two or more components (SB n , $n \geq 2$) can be detected through cross-correlation functions (CCFs) of spectra against stellar templates. Automated methods, such as DOE (Merle et al. 2017), applied to surveys like *Gaia*-ESO (Gilmore et al. 2022; Randich et al. 2022) and GALAH (De Silva et al. 2015), efficiently detect SB n . Other detection techniques have been used for SB n detection in the RAVE, GALAH, APOGEE, and LAMOST surveys, *e.g.* machine learning and Bayesian inference (Travençolo et al. 2020). A limitation of cross-correlation arises when CCFs are too wide, merging the CCF peaks of the different components into a single one. This study introduces a new method to compute CCFs using optimised spectral templates, producing significantly narrower CCFs than standard approaches.

The present study analyses only the Milky Way field stars observed with the HR10 and HR21 within the fifth internal data-release of the *Gaia*-ESO (iDR5). In total, our sample contains 160 727 spectra, corresponding to 37 565 unique Milky Way field targets. Most of the targets have at least one HR10 ($R \sim 21\,500$; [5334, 5612]Å) and one HR21 ($R \sim 18\,000$; [8475, 8983]Å) observations.

2 Methods

In Merle et al. (2017), the semi-automated tool Detection of Extrema (DOE) was applied to *Gaia*-ESO's fourth data release (iDR4) to identify spectroscopic binaries. DOE analyzes the cross-correlation function (CCF) of a spectrum to detect the number and radial velocities of stellar components by calculating the first three CCF derivatives using Gaussian kernel convolution. Local maxima and inflection points are identified to infer

¹ INAF – Osservatorio Astrofisico di Arcetri, Largo E. Fermi 5, 50125, Firenze, Italy

² Institut d'Astronomie et d'Astrophysique, Université Libre de Bruxelles, CP. 226, Boulevard du Triomphe, 1050 Brussels, Belgium

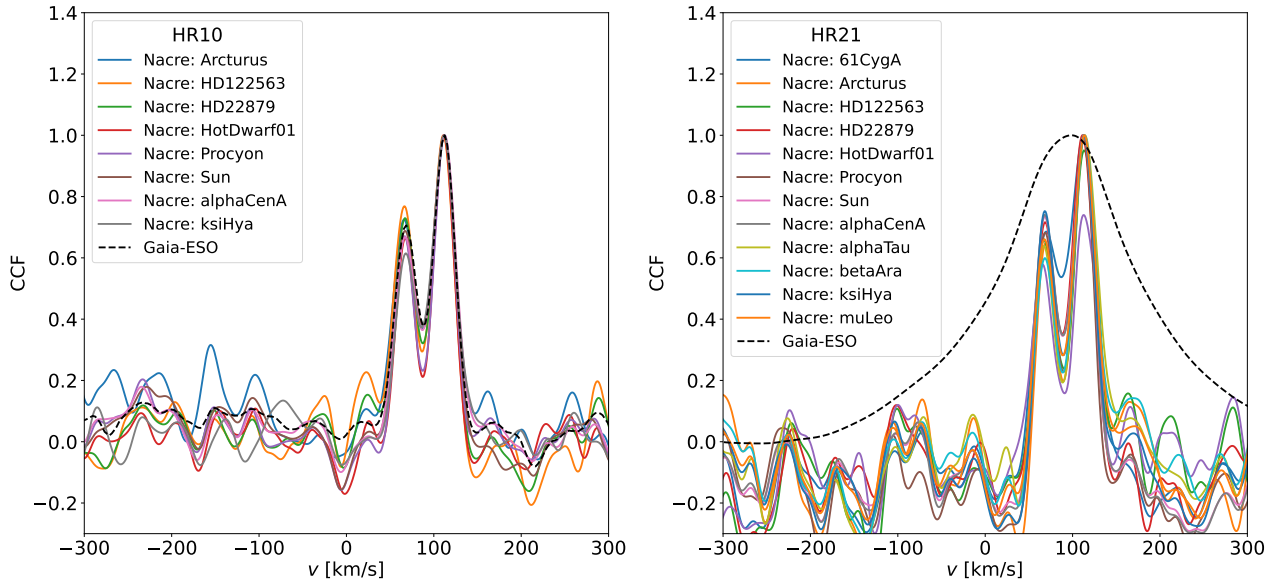


Fig. 1. Comparison of *Gaia*-ESO (dashed black line) CCFs and NACRE (other solid coloured lines) CCFs for a given HR10 (left; MJD = 56 857.311 765) and the corresponding HR21 (right; MJD = 56 856.376 009) observation of CNAME 23354061-4305405. The mask names are provided in the legend boxes.

the stellar components. The CCF is then fitted with a multi-Gaussian model to extract the velocity of each component.

When applying DOE to the iDR4 sample, we obtained puzzling cases (*e.g.* compare the black dashed lines for the HR10 and HR21 CCFs in Fig. 1) where the SB2 nature was seen in the HR10 CCF but not in the HR21 CCF. The reason is that the broad spectral features (*e.g.*, Ca II triplet) often seen in HR21 spectra tend to yield wide CCF peaks, in which more than one stellar component can be hidden. In order to obtain narrower HR21 cross-correlation functions, we noticed that a template spectrum built with only carefully selected absorption lines was a better choice, especially to ignore the very wide Ca II triplet lines in the computation. We use this approach to build about ten cross-correlating masks for HR10 and HR21. We call these new masks, NACRE masks, and the resulting CCFs are called NACRE CCFs. Figure 1 compares the GES CCFs (dashed black line) to the NACRE CCFs (coloured solid lines).

3 Results

3.1 Uncovered SB2, SB3 and SB4

Analysing the NACRE CCFs for the iDR5 sub-sample (37 565 Milky Way field stars) with DOE has given the following results: 322 SB2 (four of them being also classified as tentative SB3), 10 SB3, and two SB4. *Gaia* DR3 flags 27 stars out of the 37 260 (some targets of the iDR5 sub-sample cannot be cross-matched with the *Gaia* DR3) as non-single star (field `non_single_star` of the *Gaia* main catalogue; Gaia Collaboration et al. 2022): four are reported as eclipsing binaries (EB) and 23 as astrometric binaries (AB). None of them are identified as SB in the present study. AB might be wide long-period binaries that cannot be detected by a spectroscopic survey not designed for radial-velocity monitoring, as GES. Similarly, none of the SB2, SB3 and SB4 uncovered in this study are flagged as non-single stars by *Gaia* DR3. This shows that ground-based massive survey are still important to complement the *Gaia* spectroscopy, in particular, in the faint regime.

3.2 Mass-ratio distribution

Figure 2 shows the mass-ratio distribution for 148 out of 322 SB2. The mass ratio q can be estimated with the absolute value of the slope of the linear regression of v_s vs. v_p , where v_p and v_s are respectively the velocity of the primary and the secondary components (*e.g.* Fernandez et al. 2017). The high-quality selection (relative uncertainty on q lower than 10%) is made of 40 q estimates and has most of the q in the range $[0.7, 1.]$: it

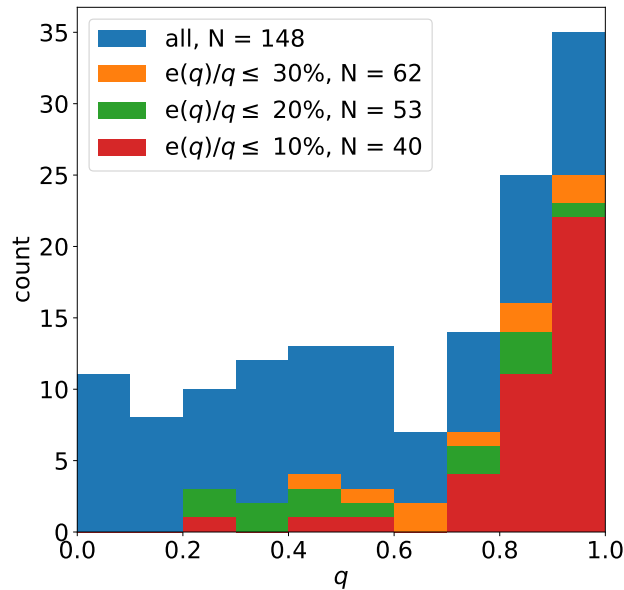


Fig. 2. Mass ratio (q) distribution for the iDR5 SB2 sample. Blue: whole sample of 148 q estimates; orange: only systems with a relative uncertainty on q lower than 30%; green: only systems with a relative uncertainty on q lower than 20%; red: only systems with a relative uncertainty on q lower than 10%. The number of systems for each cut is indicated in the legend box. The four histograms are superimposed; thus, for instance, the visible green part of the bars only shows the system with a relative uncertainty on q between 10% and 20%.

suggests that the SB2 population detected in this study mainly consists in twin stars or nearly-twin stars (*i.e.* two stars of similar mass).

3.3 Locus of SB n in the Gaia CMD

Figure 3 shows the locus of the uncovered SB n in the *Gaia* colour-magnitude diagram. We use the photometric bands of *Gaia* DR3 (Riello et al. 2021) where M_G is the absolute magnitude in the G band computed using the apparent G magnitude and the parallax, and $G_{BP} - G_{RP}$ is the colour index. We also use the estimated line-of-sight extinction and reddening given by the fields `ag_gspphot` and `ebpminrp_gspphot` in the *Gaia* source catalogue (Andrae et al. 2023) to construct the extinction-free photometric quantities, denoted by the index 0.

We note that the SB2s detected in the present paper are mainly distributed along a sequence, shifted upwards (so towards brighter magnitudes) in the uncorrected and in the extinction-corrected CMD, parallel to the main-sequence outlined by the parent sample in black. In order to estimate the mean shift between the SB2 main-sequence and the parent-sample main-sequence, we perform respectively a quadratic and quartic fit (green and blue thick lines) of these two sequences over the colour range $[0.7, 3.1]$. On the dereddened CMD, the mean difference in extinction-free absolute magnitude between each sequence, over the colour range $[0.7, 3.1]$ is 0.78 ± 0.04 mag. This should be compared to the difference of 0.75 mag expected between the absolute magnitude of an SB2 formed of two twin stars and the magnitude of each star taken separately. This finding is consistent with our previous comment on the SB2 mass-ratios: the uncovered SB2 population is made of pairs of main-sequence stars of similar mass.

References

- Andrae, R., Fouesneau, M., Sordo, R., et al. 2023, *A&A*, 674, A27
 De Silva, G. M., Freeman, K. C., Bland-Hawthorn, J., et al. 2015, *MNRAS*, 449, 2604
 Fernandez, M. A., Covey, K. R., De Lee, N., et al. 2017, *PASP*, 129, 084201
 Gaia Collaboration, Arenou, F., Babusiaux, C., et al. 2022, arXiv e-prints, arXiv:2206.05595
 Gilmore, G., Randich, S., Worley, C. C., et al. 2022, *A&A*, 666, A120
 Merle, T., Van Eck, S., Jorissen, A., et al. 2017, *A&A*, 608, A95

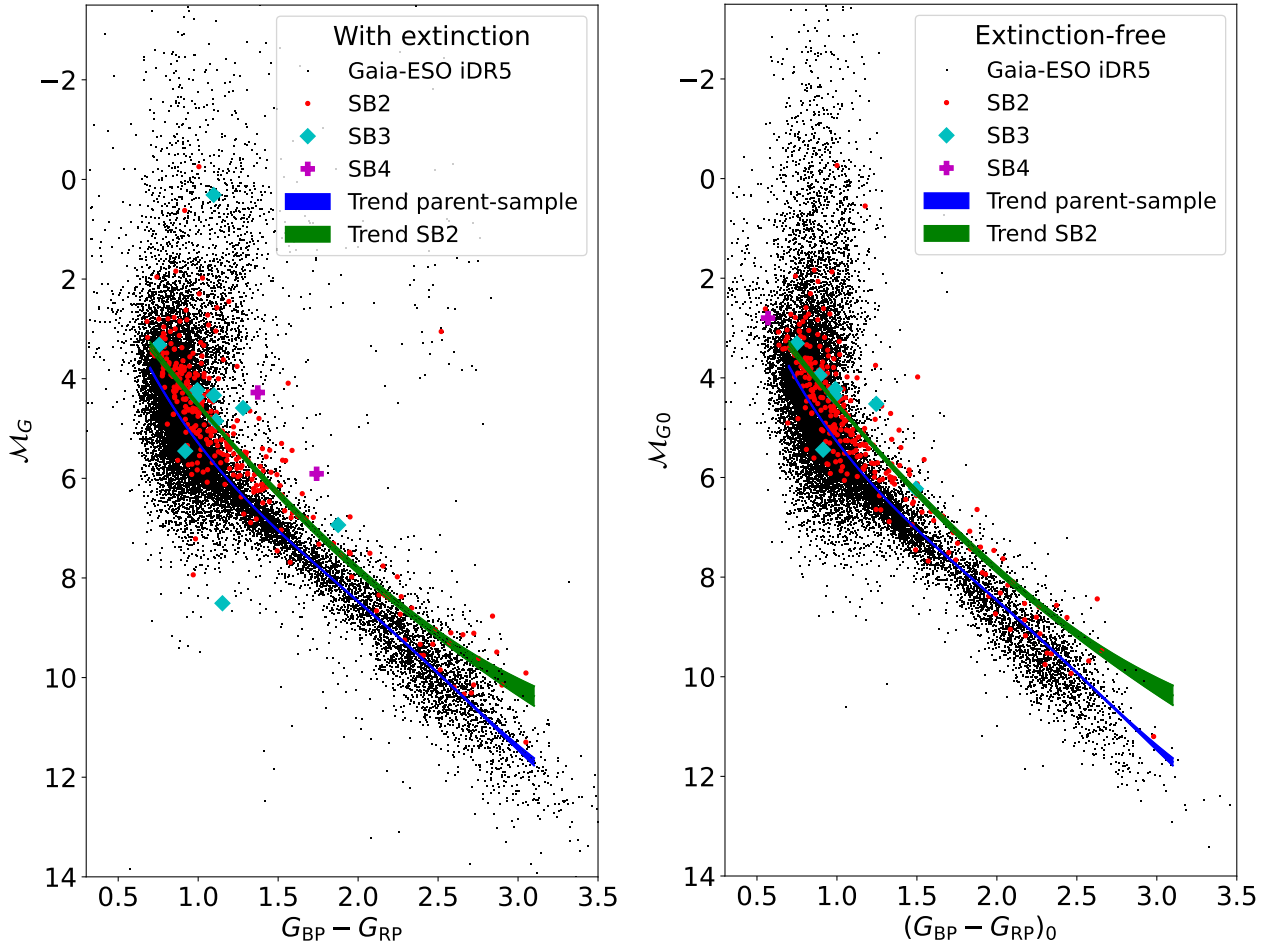


Fig. 3. Colour-magnitude diagram of the *Gaia*-ESO parent sample (black dot). Spectroscopic binaries are overplotted: SB2 (red disc), SB3 (cyan diamond), and SB4 (magenta plus). M_G is the absolute magnitude in the G band. The blue and green thick lines are respectively a quartic and quadratic fit of the rebinned parent-sample main-sequence and of the rebinned SB2 sequence. The width of the lines materialises the $1 - \sigma$ uncertainty on the locus of these two trends only due to the uncertainties on the parallaxes and photometry; the thickness of these lines is therefore not related to the vertical scatter of the datapoints. Left: photometric quantities are not corrected for the extinction. Right: photometric quantities are corrected for the extinction by using A_G and $E(G_{BP} - G_{RP})$ from *Gaia* DR3.

Randich, S., Gilmore, G., Magrini, L., et al. 2022, *A&A*, 666, A121

Riello, M., De Angeli, F., Evans, D. W., et al. 2021, *A&A*, 649, A3

Traven, G., Feltzing, S., Merle, T., et al. 2020, *A&A*, 638, A145

Van der Swaelmen, M., Merle, T., Van Eck, S., et al. 2023, arXiv e-prints, arXiv:2312.04721